Pergamon

Geochimica et Cosmochimica Acta, Vol. 66, No. 7, pp. 1221–1235, 2002

0016-7037/02 $22.00 + .00

PII S0016-7037(01)00842-0

Precise eclogitization ages deduced from Rb/Sr mineral systematics: The Maksyutov complex, Southern Urals, Russia

JOHANNES GLODNY[1,3,*], BERNARD BINGEN,[2] HÅKON AUSTRHEIM,[3] JOSÉ F. MOLINA,[3] and ANATOLIJ RUSIN[4]

[1]GeoForschungsZentrum Potsdam, Telegrafenberg C2, 14473 Potsdam, Germany
[2]Geological Survey of Norway, 7491 Trondheim, Norway
[3]Mineralogisk-Geologisk Museum, Universitetet i Oslo, Sars'gate 1, 0562 Oslo, Norway
[4]Institute of Geology and Geochemistry, Ubr RAS, Pochtovy Per. 7, Yekaterinburg 62015, Russia

(*Received January* 10, 2001; *accepted in revised form September* 17, 2001)

Abstract—The Maksyutov complex (Southern Urals, Russia) is a well-preserved example of subduction-related high-pressure metamorphism. One of its two litho-tectonic units consists of rocks that experienced eclogite-facies conditions. Published $^{40}Ar/^{39}Ar$ data on phengite, U/Pb data on rutile, and Sm/Nd mineral data define a cluster of ages around 370 to 380 Ma. Nevertheless, no consensus exists as to the detailed interpretation of data and the exact age of eclogitization. We present new, high-precision internal mineral Rb/Sr isochrons for eclogite-facies metabasites, felsic eclogites, and eclogite-facies quartz veins. Nine isochrons, mainly controlled by omphacite and white mica phases, give concordant ages with an average value of 375 ± 2 Ma (2σ). Microtextural features, such as prograde growth zoning in eclogite-facies phases, suggest that the assemblages dated formed at a stage of prograde metamorphism. Sr-isotopic equilibria among eclogite-facies phases, and among eclogite-facies fluid veins and the host rocks, indicate that our ages reflect crystallization ages, related to the prograde-metamorphic, probably fluid-mediated eclogitization reactions. This interpretation is reinforced by data from fluid-precipitated quartzitic eclogites, whose modal composition, together with intergrowth relationships, conclusively imply closed-system behavior after crystallization. The possible occurrence of a pre-375 Ma event of ultra-high-pressure metamorphism (UHPM) in the Maksyutov complex is disproved by isotope systematics, microtextures, and mineral zoning patterns.

1. INTRODUCTION

Formation of eclogites is indicative of high-pressure/low-temperature (HP/LT) stages in the metamorphic evolution of orogenic belts. Precise dating of eclogite-facies metamorphism and subsequent low-pressure/low-temperature (LP/LT) stages is crucial in understanding dynamics of orogenic systems. Exhumation rates of high-pressure metamorphic complexes can be derived from isotopic data, if precise and accurate ages can be attributed in a reliable way to both the eclogitization and the subsequent stages. Exhumation rates higher than 10 km/Ma were estimated for several high- to ultra-high-pressure (HP to UHP) metamorphic complexes, implying very rapid mass transfer during orogenic evolution (Liou et al., 1995; Gebauer et al., 1997; Amato et al., 1999).

Internal mineral isochrons derived from equilibrium mineral assemblages can potentially yield precise geochronology for segments of metamorphic PT paths. Multimineral isochrons provide control on isotopic equilibrium in the rock and thus an internal control on the validity of the age results. A prerequisite is that the basic requirements for isochron treatment of the data are strictly met, namely, a common initial isotopic ratio and a closed-system behavior after equilibration. If textural disequilibria among the minerals and indications for retrograde overprint are absent, the conditions for obtaining reliable results are likely to be fulfilled. In contrast, if evident textural disequilibria or indications for retrograde recrystallization/reequilibration are ignored when collecting data for an isochron, any age result will be questionable. For dating metamorphic events, the strategy for obtaining well-constrained age information is separation and exclusive use of minerals from the assemblage of interest. For dating of eclogite-facies metamorphism, only the minerals that are clearly related to the eclogite-facies equilibration event are useful, e.g., omphacite, garnet, and phengitic white mica. Any relict minerals of a preeclogite facies assemblage, or products of retrograde recrystallization/reequilibration are likely to introduce bias in the isochron calculation.

Possible open-system behavior of the Rb/Sr system in a rock or a mineral may be attributed either to reaction or recrystallization processes, assisted by deformation or fluid activity, or to solid-state diffusion of Sr at the mineral scale (Villa, 1998). Using this last hypothesis, Rb/Sr mineral data have been used as a tool for thermochronology in a variety of metamorphic rocks. Recent theoretical and empirical studies (Jenkin, 1997; Kühn et al., 2000) nevertheless have pointed out the limitations of the thermochronological approach as formulated by Dodson (1973), and shown that Rb/Sr mineral data have to be critically assessed taking contextual evidence into consideration, in particular the reaction history of a rock.

Although Rb/Sr mineral systematics potentially contains geochronological information on the critical stages of HP metamorphism, Rb/Sr is rarely used to date eclogite-facies rocks. This is due to analytical difficulties, possible unresolved disequilibria, or open system behavior (Gebauer, 1990). In the few well-constrained Rb/Sr data sets available, ages are mainly derived from phengite, commonly as whole-rock-phengite pairs. These ages are regarded as cooling ages (Chavagnac and

* Author to whom correspondence should be addressed (email: glodnyj@gfz-potsdam.de).

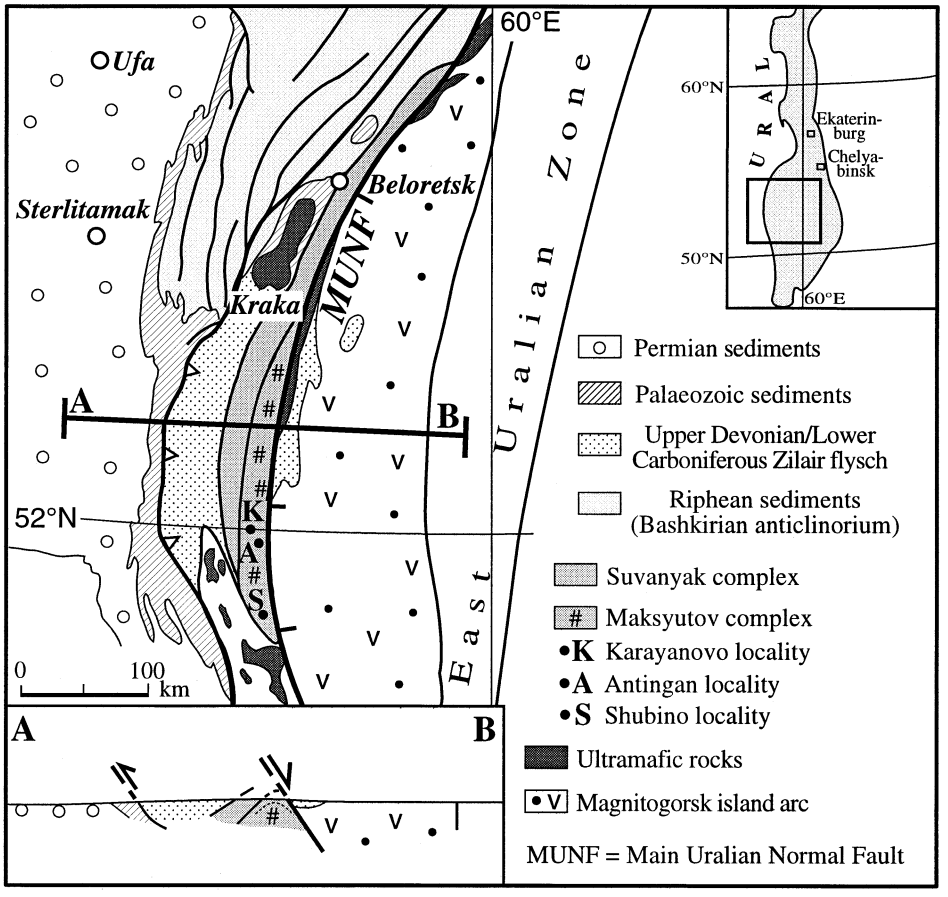

Fig. 1. Geological sketch map of the Southern Urals. Modified after Hetzel and Romer (2000).

Jahn, 1996; Ruffet et al., 1997) or recrystallization ages (Amato et al., 1999). Interpretations of data as crystallization ages are discussed only if peak metamorphic temperatures were at and below 550°C (Inger et al., 1996; Sherlock et al., 1999).

In this study we revisit the HP Maksyutov complex, Southern Urals, Russia, for which consensus is lacking as to the exact timing of eclogite-facies metamorphism and exhumation. Rb/Sr isochron ages are derived from white micas and associated eclogite-facies minerals. We will show that internal isochrons give a reliable estimate of the timing of the eclogitization reactions. Implications for the evolution of the Maksyutov complex are then discussed.

2. GEOLOGICAL FRAMEWORK

The Uralian orogenic belt formed by collision of the East European Platform with an assemblage of Siberian-Kazakhian terranes in Devonian to Triassic time (Hamilton, 1970; Zonenshain et al., 1984). The Main Uralian Fault, separating rocks of the East European Platform from microcontinents and island arcs further east, is commonly regarded as the main suture zone of the orogen. Several blueschist and eclogite-facies metamorphic complexes occur as a discontinuous belt in the footwall of the east-dipping suture (Dobretsov and Sobolev, 1984; Sobolev et al., 1986).

The HP Maksyutov complex is ~200 km long and up to 20 km wide, trending N-S along the main axis of the Uralian orogen (Fig. 1). It is bounded by tectonic contacts (Echtler and Hetzel, 1997) and essentially surrounded by low-grade or unmetamorphic rocks. The complex is bounded to the east by the Main Uralian Normal Fault (Echtler and Hetzel, 1997), juxtaposing it beneath a tectonic melange with ophiolitic components, and rocks of the Devonian calc-alkaline Magnitogorsk island arc. The western limit is made up by the overlying Suvanyak complex, a succession of Ordovician to Devonian greenschist facies passive margin sediments (Echtler, 1998 and references therein). The Suvanyak and Maksyutov complexes constitute an antiformal structure, termed the Uraltau ridge (Ivanov et al., 1975). The Maksyutov complex is an exceptionally well-preserved example of subduction-related HP metamorphism (Ernst et al., 1995; Hetzel et al., 1998). Indications for significant late-orogenic thermal or magmatic overprint are absent. Therefore, the exhumation of the Maksyutov complex is not related to orogenic collapse or postorogenic extension (Berzin et al., 1996). Instead, an exhumation mechanism involving syncollisional normal faulting was proposed (Echtler and Hetzel, 1997).

The Maksyutov complex consists of two tectonometamorphic units (Lennykh et al., 1995; Dobretsov et al., 1996), as defined by the peak metamorphic grade. The structurally lower, eclogite-facies, gneissic unit #1, which is the target of this

Table 1. Compilation of published age data for eclogite-facies metamorphism in unit #1 of the Maksyutov complex.

Method	Material, Approach	Age (Ma)	MSWD	Nd (init.)	Data source
Sm/Nd	mineral isochron	399 ± 35	10.5	0.51240 ± 4	Beane and Connelly, 2000
Sm/Nd	rutile + apatite	382 ± 10	–	–	″
U/Pb	rutile + apatite, U/Pb	377 ± 2	2.1	–	″
U/Pb	rutile, U/Pb isochron	384 ± 4	–	–	″
$^{40}Ar/^{39}Ar$	5 phengite samples	377 ± 2 to 372 ± 2	–	–	″
Sm/Nd	mineral isochron	396 ± 57	11	0.51207 ± 12	Shatsky et al., 1997
Sm/Nd	mineral isochron	375 ± 3	0.2	0.51236 ± 2	″
Sm/Nd	mineral isochron	366 ± 7	0.98	0.51236 ± 2	″
Sm/Nd	mineral isochron	357 ± 15	3	0.51253 ± 3	″
$^{40}Ar/^{39}Ar$	phengite	375.4 ± 3.4	–	–	Lennykh et al., 1995
$^{40}Ar/^{39}Ar$	phengite	377.7 ± 3.8	–	–	Matte et al., 1993
$^{40}Ar/^{39}Ar$	phengite	372.9 ± 3.8	–	–	″
$^{40}Ar/^{39}Ar$	phengite	387.9 ± 4.0	–	–	″

Errors are reported at the 2σ level. Sample sites of Beane and Connelly (2000): Maksyutovo, Karayanovo, Shubino, Novopakrova. Sample site for all other material: Sakmara river bank near Karayanovo, or not stated precisely.

study, is predominantly composed of micaceous, quartzitic ± graphitic, continent-derived metasediments. Local layers or boudins of mafic eclogites presumably represent former mafic dykes. This association of rocks is interpreted as mainly Proterozoic upper continental crust of the East European passive margin (Hetzel, 1999). Protolith ages for this unit are estimated at between ~800 and 1830 Ma, based on Rb/Sr whole rock data, and U/Pb zircon data from interlayered metavolcanics (Dobretsov, 1974; Dobretsov and Sobolev, 1984; Sobolev et al., 1986; Valizer and Lennykh, 1988). The unit #1 experienced eclogite-facies metamorphism at minimum pressures of 1.5 GPa to 2.1 GPa (Beane et al., 1995; Dobretsov et al., 1996; Hetzel et al., 1998; Schulte and Blümel, 1999) and temperatures of ~500 to 600°C (Hetzel et al., 1998; Schulte and Blümel, 1999). A later blueschist to greenschist facies overprint is locally observed (Lennykh et al., 1995). The P,T estimates are similar for different sampling sites near the villages of Karayanovo, Antingan, and Shubino (Fig. 1). Some potential indications for an early stage of UHP metamorphism, mainly possible quartz and graphite pseudomorphs after coesite and diamond, have been reported (Dobretsov et al., 1996; Leech and Ernst, 1998; Leech and Stockli, 2000; Leech and Ernst, 2000).

The upper unit #2 experienced greenschist to blueschist facies metamorphism at much lower peak metamorphic pressures (0.5 to 0.6 GPa; Lennykh et al., 1995; <0.8 GPa, <450°C, Hetzel et al., 1998). Consequently, eclogites are absent in unit #2.

3. PUBLISHED AGE DATA AND INTERPRETATIONS

Most published ages for metamorphism of the Maksyutov complex cluster around 370 to 380 Ma (Table 1). However, no consensus exists on the precise interpretation of these data, mainly due to problems inherent to the dating methods.

All errors on both published and new dates are reported as 2σ throughout this paper.

$^{40}Ar/^{39}Ar$ ages of phengite range from 388 ± 4 to 372 ± 2 Ma (Matte et al., 1993; Lennykh et al., 1995; Beane and Connelly, 2000). Interpretation of ^{40}Ar-^{39}Ar data from high-pressure phases can be difficult for two reasons. From multi-isotope studies (Li et al., 1994; Ruffet et al., 1997) as well as from $^{40}Ar/^{39}Ar$ laser probe work (Ruffet et al., 1995; Reddy et al., 1996), it is known that virtually undetectable excess Ar may be present in HP phengites, and geologically meaningless ages may be generated despite systematic $^{40}Ar/^{39}Ar$ plateau ages (Ruffet et al., 1997). In cases where excess Ar can be excluded, $^{40}Ar/^{39}Ar$ dating of eclogite-facies phases may yield analytically precise results, but the geologic interpretation of the age values remains problematical. This is mainly due to controversy about Ar loss mechanisms and blocking temperatures of datable phases (Villa, 1998). Thus, while Matte et al. (1993) interpret their ages as dating a stage close to the peak of HP metamorphism, Lennykh et al. (1995) refer to a blocking temperature of 350°C for K/Ar in white mica. Consequently, the latter authors interpret their data as cooling ages, dating an exhumation/thermal relaxation stage, and state that eclogite-facies metamorphism occurred before 370 to 380 Ma.

U/Pb data on rutile have yielded two ages at 384 ± 4 and 377 ± 2 Ma (Beane and Connelly, 2000). These are difficult to interpret due to uncertainty in the closure temperature for the U/Pb system in rutile. Estimates for the closure temperature range between ca. 420°C (Mezger et al., 1989) and around 600°C (Cherniak, 2000).

The published Sm/Nd mineral isochrons yield age values between 399 ± 35 and 357 ± 15 Ma (Shatsky et al., 1997; Beane and Connelly, 2000). Dating of eclogites by the Sm/Nd-method may be problematic due to possible inheritance (Jagoutz, 1995; Miller and Thöni, 1997). For isotopically incompletely equilibrated assemblages, isochron calculation may yield spurious results.

The age data summarized above have inspired contrasting models of the tectonometamorphic and geodynamic evolution of unit #1 in the context of an arc-continent collision, in the Devonian (Matte et al., 1993; Lennykh et al., 1995; Matte and Chemenda, 1996; Dobretsov et al., 1996; Echtler and Hetzel, 1997; Beane, 1997b; Chemenda et al., 1997; Brown et al., 1998; Hetzel et al., 1998; Hetzel, 1999; Beane and Connelly, 2000; Leech and Ernst, 2000). For example, Lennykh et al. (1995) infer peak metamorphism at a time *before* 370 to 380 Ma and passage of the rocks through the 350°C isotherm at 370 to 380 Ma. Beane and Connelly (2000), and Matte et al. (1993) interpreted the data in terms of metamorphism, rapid exhuma-

tion and cooling *at* 370 to 380 Ma. Dobretsov et al. (1996), Leech and Ernst (2000), and Leech and Stockli (2000) postulate a possible early stage of UHP metamorphism before ca. 380 to 400 Ma.

These limitations of the geochronological methods applied so far, together with the considerable range of ages and their controversial interpretation, stimulated the present study.

4. SAMPLING AND PETROGRAPHY

Continuous debate centers on the mechanisms and relevant distances for Sr and Nd isotopic rehomogenization during metamorphic events (Villa, 1998). Therefore, we have chosen to work with small, lithologically homogeneous samples of ~10 to 100 g. The smaller the sample is, the more likely it is that isotopic rehomogenization during metamorphism was effective throughout. In larger samples, premetamorphic compositional variations may result in Sr and Nd isotopic contrasts of a scale too large to be erased by the metamorphism. By preparation of minerals from sufficiently small samples, we avoid bias arising from mixing of minerals from domains with different initial $^{87}Sr/^{86}Sr$ values.

Except for retrograde shear and fracture zones, the eclogites are well preserved. Textures are variable. Some samples exhibit prograde fabrics, like high-pressure foliation defined by glaucophane-omphacite and overgrown by garnet (Hetzel et al., 1998). Other samples show equilibrium crystallization textures. The eclogite mineralogy is variable and depends on the whole rock chemistry. Locally, glaucophane-bearing assemblages are observed. The variable assemblages do not imply significant differences in PT conditions. There is evidence for glaucophane stability at eclogite-facies conditions, and for simultaneous formation of glaucophane-bearing and glaucophane-free assemblages during the same event (Hetzel et al., 1998).

Nine samples of white mica-bearing eclogite-facies rocks, some of which contain glaucophane, were selected for this study. The samples were collected in unit #1, near the villages of Karayanovo, Antingan, and Shubino (Fig. 1). The detailed petrography of the samples is summarized in the Appendix. Sample 22E is a fluid-precipitated, eclogite-facies quartzitic vein. Sample 23D is a quartzite. The eclogite-facies assemblages comprise garnet + omphacite + epidote/zoisite + phengite + rutile ± kyanite ± zircon ± apatite ± quartz ± glaucophane ± paragonite. Evidence for posteclogite facies crystal-plastic deformation is absent in our sample set, but some samples exhibit retrogression products. Retrograde phases are sphene (as rims around rutile), albite, chlorite, small (<30 μm) phengite, blue amphibole, and actinolite. Retrogression is confined to zones around small fractures which acted as fluid pathways. Consequently, most of the retrograde reactions were induced by introduction of free fluids under blueschist to greenschist-facies conditions. This is in accordance with other descriptions of the alteration patterns (Beane et al., 1995; Dobretsov et al., 1996; Shatsky et al., 1997; Hetzel et al., 1998; Schulte and Blümel, 1999). It is important to note that, apart from the sparse retrogression sites, the main volume of the samples is characterized by complete absence of free fluids after the eclogitization reactions.

Special attention was paid to the white mica population, because their relationships to other minerals and their composition are decisive for the interpretation of Rb/Sr data. Electron microprobe analyses were performed on white micas and associated minerals. A set of representative white mica analyses is presented in Table 2.

Phengite has 3.20 to 3.47 Si per formula unit (11 O,OH) and a paragonite component of up to 20 mol-%. Some phengite grains, for example in samples 22E and 31A (Table 2, No. 3 to 8) show internal zoning, with increasing celadonite component toward the rims. Phengite grains coexisting with paragonite also show a decrease in the Na/Na + K ratios toward the rim. These features are indicative for *increasing pressures* during mica crystallization (Guidotti et al., 1994) and imply contemporaneous growth of paragonite and phengite. The eclogite of sample 22B is crosscut by a quartzitic vein (sample 22E). Whereas the phengite in the vein shows zoning (Table 2, No. 3, 4), the phengite in the surrounding eclogite is unzoned, and has a composition similar to that of the rim of phengites in the vein (Table 2, No. 1, 2). In sample 23B, which shows some retrogression, it is possible to identify two distinct phengite generations. Primary, eclogite-facies phengite has an average grain size >100 μm. A second generation of alteration-related, small (~30-μm) phengite grains is located in albite + chlorite + phengite aggregates that occur as tiny (diameter ~50 μm) veinlets and along grain boundaries. Analysis of both generations revealed similar chemical compositions, with some compositional variability among different primary grains. A significant difference is that phengite of the second generation has higher Fe/Fe + Mg ratios (Table 2, No. 10 to 12). In the garnet-rich sample 31A, garnet is commonly present in atoll-shaped grains and carries abundant phengite inclusions. The phengite of this sample has the highest Si p.f.u. found in the sample set. Phengite grains show prograde core- to rim zoning, irrespective of their textural position: Phengite enclosed in garnet is chemically identical to phengite in the matrix (Table 2, No. 5 to 9)

Paragonite is abundant as inclusions in garnet, but also occurs as a matrix phase and in intergrowth relationship with phengite (Table 2, No. 13 to 15). Its chemical composition is close to the ideal endmember, with Na/Na + K atomic ratios of 0.9 to 0.95. The Sr content of paragonite is remarkably high (>2500 ppm, see sample 22F, Table 3)

Garnet in most samples contains numerous inclusions, and commonly displays prograde chemical core to rim zoning, with decreasing Mn and increasing Mg contents (Schulte and Blümel, 1999). Among the inclusion phases are epidote/zoisite, glaucophane, rutile, quartz, chlorite, phengite, omphacite, lawsonite, albite, actinolite, paragonite, sphene, a (Ba, Sr)-sulfate phase, stilpnomelane, and apatite. The zoning pattern and the spectrum of inclusions, in particular the occurrence of lawsonite, together indicate that prograde features of the garnet are preserved.

Epidote is usually zoned, with (light rare earth element [LREE], Mn)-rich cores. The Mn zoning pattern resembles the Mn distribution in garnet, implying that epidote cores grew contemporaneously with garnet cores in an early stage of the eclogitization reaction sequence. Sr distribution in epidote is heterogeneous. In patches, very high SrO contents of up to 5.5% are found, interpreted as evidence for prograde growth (Nagasaki and Enami, 1998)

Other phases also show core to rim zoning indicating growth

Table 2. Representative electron microprobe analyses of white mica phases from different structural settings, unit #1, Maksyutov complex.

Point#	1	2	3	4	5	6	7	8	9	10	11	12	13	14	15
Sample	22B	22B	22E	22E	31A	31A	31A	31A	31A	23B	23B	23B	25B	25B	27B
Phase	phengite	phengite	phengite	phengite	phengite	phengite	phengite	phengite	phengite	phengite	phengite	phengite	phengite	paragonite	paragonite
Notes	core	rim	core	rim	core	rim	core	rim	core	big grain #2	big grain #6	fine flake	intergrown	intergrown	grain incl.
Struct. Pos.	matrix	matrix	qtz vein	qtz vein	garnet	garnet	atoll garnet	atoll garnet	matrix	ecl. matrix	ecl. matrix	alteration	with pg	with phengite	in grt core
SiO_2 (wt-%)	49.19	49.41	47.83	49.61	50.27	50.72	50.32	51.02	50.93	50.03	48.70	46.06	49.44	46.88	46.73
TiO_2	0.35	0.37	0.67	0.50	0.53	0.47	0.58	0.48	0.55	0.18	0.69	0.13	0.23	0.07	0.03
Al_2O_3	27.59	27.41	28.69	27.45	25.45	24.85	24.46	24.37	25.11	25.08	27.97	26.13	28.04	39.78	40.14
FeO	3.96	3.91	3.74	3.36	3.12	2.84	3.44	3.03	2.83	3.45	3.31	8.22	1.58	0.17	0.44
MnO	0.09	0.04	0.05	0.01	0.01	0.04	0.00	0.00	0.00	0.05	0.00	0.01	0.00	0.00	0.00
MgO	3.02	3.13	2.75	3.18	4.02	4.02	4.26	4.31	4.14	3.56	2.98	3.39	2.58	0.14	0.16
CaO	0.07	0.00	0.00	0.01	0.01	0.08	0.04	0.06	0.00	0.00	0.00	0.06	0.01	0.28	0.32
Na_2O	0.92	0.81	1.06	0.73	0.26	0.18	0.33	0.25	0.26	0.20	0.73	0.31	0.37	7.44	7.55
K_2O	10.69	10.37	10.07	10.52	10.97	10.84	10.91	11.34	10.61	11.15	10.56	10.59	10.66	0.98	0.60
	95.89	95.44	94.86	95.38	94.65	94.04	94.34	94.86	94.43	93.71	94.94	94.89	92.91	95.73	95.96
Si	3.31	3.33	3.24	3.34	3.41	3.45	3.43	3.46	3.44	3.43	3.29	3.22	3.37	2.99	2.97
Ti	0.02	0.02	0.03	0.03	0.03	0.02	0.03	0.02	0.03	0.01	0.04	0.01	0.01	0.00	0.00
Al	2.19	2.18	2.29	2.18	2.03	1.99	1.97	1.95	2.00	2.03	2.23	2.15	2.26	2.99	3.01
Fe	0.22	0.22	0.21	0.19	0.18	0.16	0.20	0.17	0.16	0.20	0.19	0.48	0.09	0.01	0.02
Mn	0.01	0.00	0.00	0.00	0.00	0.00	0.00	0.00	0.00	0.00	0.00	0.00	0.00	0.00	0.00
Mg	0.30	0.31	0.28	0.32	0.41	0.41	0.43	0.44	0.42	0.36	0.30	0.35	0.26	0.01	0.02
Ca	0.01	0.00	0.00	0.00	0.00	0.01	0.00	0.00	0.00	0.00	0.00	0.00	0.00	0.02	0.02
Na	0.12	0.11	0.14	0.10	0.03	0.02	0.04	0.03	0.03	0.03	0.10	0.04	0.05	0.92	0.93
K	0.92	0.89	0.87	0.90	0.95	0.94	0.95	0.98	0.92	0.98	0.91	0.94	0.93	0.08	0.05
Cel (Si-3)	0.31	0.33	0.24	0.34	0.41	0.45	0.43	0.46	0.44	0.43	0.29	0.22	0.37		
Fe/Fe + Mg)	0.42	0.41	0.43	0.37	0.30	0.28	0.31	0.28	0.28	0.35	0.38	0.58	0.26	0.40	0.61
Na/(Na + K)	0.12	0.11	0.14	0.10	0.03	0.02	0.04	0.03	0.04	0.03	0.10	0.04	0.05	0.92	0.95

Struct. Pos.: describes microstructural setting. Analytical conditions: Cameca Camebax instrument, Univ. of Oslo; acceleration voltage 15 kV; beam current 10 nA for mica, 20 nA for other phases; defocussed beam for mica and omphacite. Mica stoichiometry was calculated on the basis of 11 (O,OH) per formula unit.

Table 3. Rb/Sr analytical data.

Sample No., Analysis No.	Material	Rb (ppm)	Sr (ppm)	$^{87}Rb/^{86}Sr$	$^{87}Sr/^{86}Sr$	$^{87}Sr/^{86}Sr$ 2σ (%)
22B (Shubino) 376.5 ± 3.7 Ma						
OS62	omphacite	0.06	25.64	0.0070	0.703833	0.0078
OS2	white mica	187.09	66.62	8.1567	0.747550	0.0031
OS63	glaucophane	1.64	18.40	0.2583	0.705137	0.0032
22F (Shubino) 378.5 ± 4.7 Ma						
OS59	epidote	0.18	6097.58	0.0001	0.703815	0.0030
OS61	omphacite	0.27	35.13	0.0221	0.703944	0.0034
OS3	white mica 1 (phn)	190.59	554.51	0.9946	0.709182	0.0023
OS4	white mica 2 (pg)	6.77	2673.38	0.0073	0.703868	0.0033
22E (Shubino) 375.2 ± 3.8 Ma						
OS64	apatite	0.06	839.43	0.0002	0.703770	0.0029
OS65	epidote	0.39	2823.92	0.0004	0.703787	0.0023
OS1	white mica	167.4	176.81	2.7422	0.718424	0.0027
23B (Shubino) 372.4 ± 3.8 Ma						
OS58	epidote (*)	0.18	3497.25	0.0001	0.704945	0.0012
OS7	white mica	228.4	187.08	3.5374	0.722565	0.0028
PS79	omphacite	0.55	96.40	0.0164	0.703898	0.0055
PS83	glaucophane (*)	0.62	5.70	0.3124	0.705955	0.0014
PS128	whole rock (*)	25.82	269.08	0.2775	0.705918	0.0022
23D (Shubino) 375.5 ± 2.2 Ma						
PS159	white mica 1	397.15	62.31	18.6285	0.811847	0.0014
OS8	white mica 2	386.64	62.27	18.1436	0.810181	0.0032
PS129	whole rock	132.81	76.82	5.0174	0.739186	0.0018
OS56	omphacite	0.09	2.62	0.1007	0.713029	0.0023
OS57	glaucophane (*)	0.42	4.83	0.2516	0.713342	0.0037
27B (Antingan) 372 ± 15 Ma						
OS5	white mica 1	35.88	395.19	0.2626	0.706800	0.0028
OS6	white mica 2	8.01	712.81	0.0325	0.705582	0.0024
PS127	whole rock (*)	3.13	94.29	0.0960	0.706235	0.0016
29 (Antingan) 373.8 ± 3.9 Ma						
OS10	white mica	174.81	25.71	19.8743	0.810830	0.0040
PS126	whole rock	2.67	153.67	0.0502	0.705962	0.0016
OS54	glaucophane	0.22	3.48	0.1804	0.706706	0.0100
OS53	epidote	0.19	1238.29	0.0004	0.705727	0.0027
OS55	omphacite	0.18	8.72	0.0610	0.706190	0.0174
25B (Karayanovo) 377.7 ± 7.3 Ma						
OS60	omphacite	0.35	51.23	0.0198	0.704927	0.0027
OS11	paragonite	4.34	1198.93	0.0105	0.704900	0.0031
PS63	mixed white mica	25.21	1108.06	0.0658	0.705187	0.0014
PS62	phengitic w. mica	119.21	714.48	0.4827	0.707429	0.0012
31A (Karayanovo) 374.3 ± 2.7 Ma						
PS87 (*)	apatite	1.31	3581.97	0.0011	0.703577	0.0010
PS64	white mica 1	230.91	71.49	9.3877	0.753907	0.0009
PS125	omphacite	9.32	119.79	0.2251	0.704938	0.0024
PS123	white mica 2	231.14	69.31	9.6934	0.755242	0.0016

Errors are reported at the 2σ level. (*): not used for age calculation. An uncertainty of ±1% has to be assigned to Rb/Sr ratios.

22F white mica 1: Frantz magnetic at 0.5 A/13°, 125–250 μm; 22F white mica 2: Frantz magnetic at 0.9 A/13°; 23D white mica 1: Frantz magnetic at 0.7 A/13°; 23D white mica 2; Frantz magnetic at 0.6 A/13°; 25B mixed white mica 355–500 μm; 25B phengitic white mica 355–500 μm; 27B white mica 1: density <2.96; 27B white mica 2: density >2.96, Frantz magnetic at 1.5A/13°; 29, white mica: Frantz magnetic at 0.7A/13°, 80–160 μm; 31A, white mica 1: Frantz nonmagnetic at 0.56A/13°, >250 μm; 31A, white mica 2: Frantz magnetic at 0.56A/13°, >250 μm.

at increasing pressures: Some amphibole is zoned from barroisite cores toward glaucophane rims. Omphacite in most cases has no zoning, but in the zoned crystals, jadeite component increases toward the rim.

In summary, and in line with the findings of Hetzel et al. (1998), there is abundant evidence for preservation of prograde-metamorphic features in rocks that escaped from strain or fluid activity along the retrograde metamorphic evolution.

5. ANALYTICAL PROCEDURES

For the purpose of Rb/Sr and Sm/Nd isotope analyses, mineral concentrates of the different white micas, omphacite, glaucophane, apatite, and epidote/zoisite were produced. Care was taken to avoid material altered by weathering or reflecting posteclogite-facies fluid–rock interaction. White mica sieve fractions (all larger than 80 μm, to exclude small, retrogression-related crystals from analysis) were ground in pure ethanol in an agate mortar and then sieved in ethanol to obtain inclusion-free separates. Secondary (Fe, Mn)-hydroxides on some omphacite and glaucophane separates were removed with a 5% aqueous solution of oxalic acid as they are likely to adsorb contaminants. The concentrates were purified by hand-picking under the binocular microscope. Whole rock powders were prepared in an agate mill.

Samples were analyzed for Rb, Sr, Sm, and Nd contents by isotope dilution. They were weighed into Savillex screw-top containers, spiked with suitable mixed ^{87}Rb,^{84}Sr (^{149}Sm, ^{150}Nd) spike solutions, and dissolved in a mixture of HF and HNO_3. Solutions were processed by standard cation-exchange techniques. Determinations of Sr isotope ratios were carried out on a VG Sector 54 multicollector thermal ionization mass spectrometer (TIMS) (GeoForschungsZentrum Potsdam) in dynamic mode. For some samples, analyses were performed on a Finnigan MAT 262 TIMS (Mineralogical Geological Museum, University of Oslo) in static mode. The values obtained for $^{87}Sr/^{86}Sr$ of the NBS standard SRM 987 during the period of analytical work were 0.710263 ± 0.000010 (n = 16) for the Potsdam instrument and 0.710170 ± 0.000015 (n = 14) for the Oslo instrument. From the systematic deviation, a correction factor was determined and applied to the results of the static mode analyses. All isotopic ratios were normalized to an $^{86}Sr/^{88}Sr$ ratio of 0.1194. Rb analyses were done on a VG Isomass 54 single collector TIMS instrument at the GeoForschungsZentrum Potsdam. The observed ratios were corrected for 0.25% per a.m.u. mass fractionation. Total procedural blanks were consistently below 0.15 ng for both Rb and Sr. Due to highly variable blank values, a useful blank correction is not applicable. For age calculations, an uncertainty of ± 1%, as derived from replicate analyses of natural mica samples, is assigned to the $^{87}Rb/^{86}Sr$ ratios. $^{87}Sr/^{86}Sr$ ratios are reported with their 2σ internal precision plus uncertainties from spike correction. For calculation of isochron parameters, a standard error of ± 0.005% for $^{87}Sr/^{86}Sr$ ratios was applied if individual errors were smaller than this value. This error estimate (2σ) was derived from reproducibility tests for Sr isotope ratios on the two instruments used. The program Isoplot/Ex 2.06 (Ludwig, 1999) was used to calculate regression lines. Sm, Nd isotope analyses were carried out on a Finnigan MAT 262 mass spectrometer at the GeoForschungsZentrum Potsdam. Nd was analyzed in dynamic, Sm in static mode. For calculations, standard errors of ± 0.003% for $^{143}Nd/^{144}Nd$ ratios and ± 0.5% for $^{147}Sm/^{144}Nd$ ratios were assigned to the results.

6. RESULTS

6.1. Rb/Sr

The Rb/Sr results on the nine samples are reported in Table 3, Figures 2a and 2b and are summarized in Figure 3. Within limits of errors, the Rb/Sr isochron ages are all identical at around 375 Ma, irrespective of sampling site, bulk chemistry and mineral assemblage. A mean age value of 375.1 ± 1.2 Ma (classical weighted average) or 375.1 ± 1.8 Ma (Tukey's Biweight Mean) is obtained. Apart from the age information, this average calculation illustrates both accuracy and reproducibility of the data produced with two separately calibrated sets of spikes in two different laboratories.

Some data, indicated by asterisks in Table 3, were excluded from the age calculation for different reasons. Some glaucophane analyses (samples 23B and 23D) seem unreliable due to very low concentrations of Rb and Sr and small sample sizes, resulting in potentially too low sample/blank ratios. Disequilibrium was observed in three of the samples, corresponding to evidence of postpeak metamorphic retrograde reactions in the rock (see Appendix). In these cases, only minerals clearly belonging to the eclogite-facies assemblage (e.g., omphacite, phengite) were used for age calculations. The fact that omphacite and white mica (paragonite, phengite) yield identical ages in all samples indicates that in some samples subjected to retrogression the Rb/Sr systems of apatite (31A), epidote (23B), and whole rock (23B, 27B) were slightly modified.

For the majority of the samples, comparatively primitive initial $^{87}Sr/^{86}Sr$ ratios between 0.7037 and 0.7058 were found. A higher ratio of 0.7125 is obtained for sample 23D which is a quartz-rich metasedimentary lithology.

6.2. Sm/Nd

The results of the Sm/Nd analyses are presented in Table 4. Only sample 23D (Shubino) yielded sufficient spread in Sm/Nd ratios for calculation of an age value. This sample yields an apparent age of 416 ± 26 Ma, which is not in agreement with the age derived from the Rb/Sr dataset.

7. DISCUSSION

7.1. Rb/Sr Mineral Isochrons—Closure or Crystallization Ages?

The key problem in interpreting Rb/Sr mineral data is whether the isochron ages reflect the crystallization of the mineral assemblage or cooling through a blocking temperature. In the original model of thermochronology formulated by Dodson (1973), the closure temperature (T_c) is related to the solid-state diffusion parameters of the mineral, its effective grain size, and the cooling rate, i.e., the temperature history. It is independent of the matrix surrounding the mineral, as the matrix is modeled as an infinite reservoir in which diffusion is fast. In rocks evolving in closed system, i.e., in the absence of free fluids, this assumption is not fulfilled and at best approached if a Sr-rich, modally abundant mineral can act as a large reservoir in the rock, for example feldspar. More elaborated isotope mobility models by Giletti and Farver (1988), Giletti (1991), Jenkin et al. (1995), and Jenkin (1997) show that the exchange of Sr isotopes is dependent on the modal proportions of minerals, intergrowth relationships, and on the Sr diffusion kinetics of all minerals of an assemblage. For example, in bimineralic rocks the effective closure for diffusion is determined by the mineral with the higher T_c. For rocks made up of a mixture of feldspars and micas, the apparent T_c of micas is generally higher than the T_c predicted by the model of Dodson (1973). In eclogites, feldspars are not part of the mineral assemblages. Therefore, the potential of the eclogite-facies mineral matrices to act as Rb, Sr exchange reservoirs has to be evaluated. In this study, Rb/Sr mineral ages are derived from two types of eclogite-facies matrices: omphacite + garnet ± glaucophane ± epidote/zoisite matrix and quartz-rich matrix. Several lines of evidence indicate that these ages, mainly controlled by white mica, are not affected by significant postcrystallization open system behavior and thus can be interpreted as crystallization ages.

In the omphacite + garnet ± glaucophane ± epidote/zoisite matrix, the main Sr-bearing minerals are omphacite, epidote/zoisite, and phengite. Other phases are either accessories (apatite) or do not carry significant Sr (quartz, rutile, glaucophane, garnet). Interpretation of a Rb/Sr phengite age as a cooling age

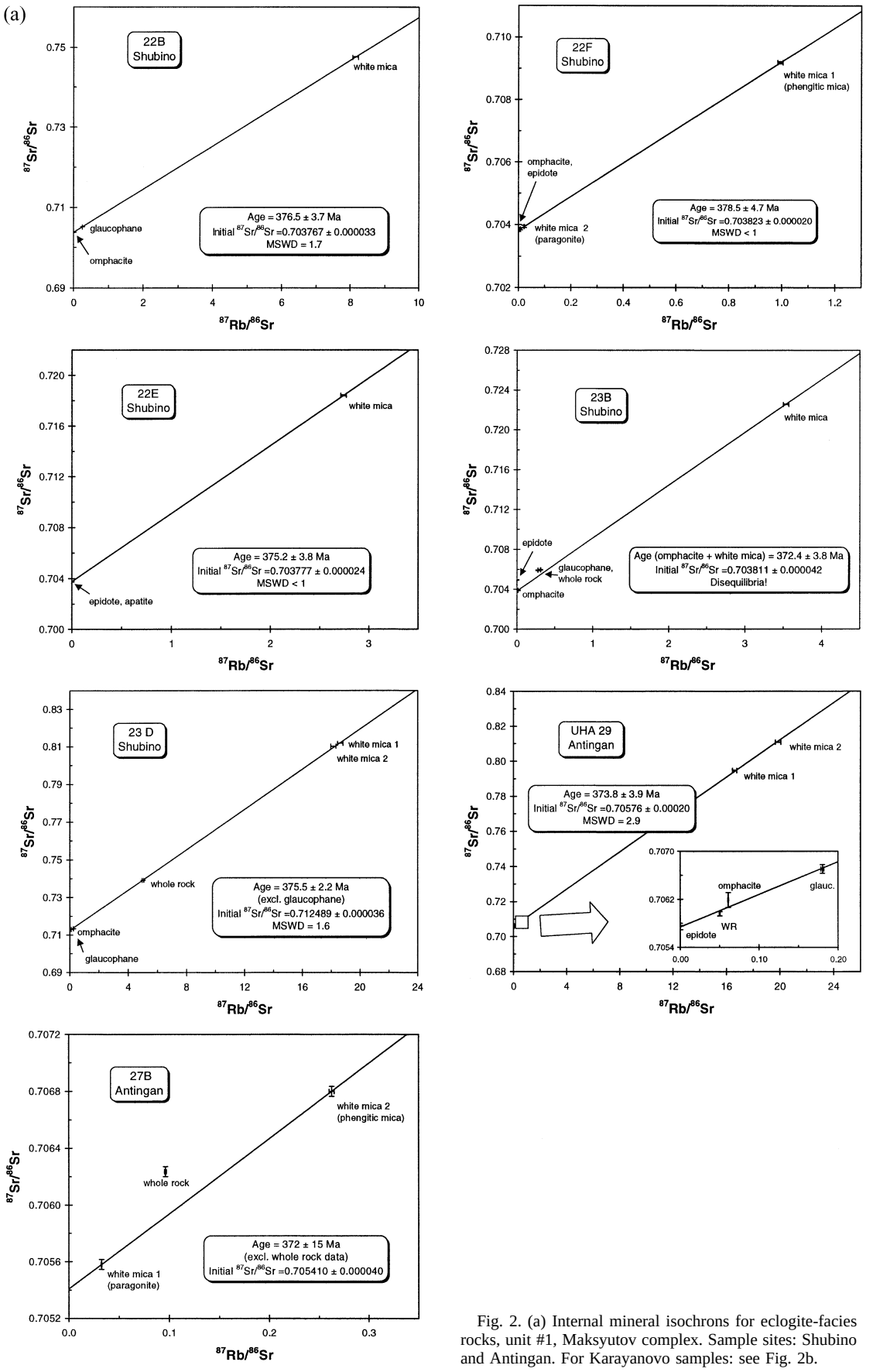

Fig. 2. (a) Internal mineral isochrons for eclogite-facies rocks, unit #1, Maksyutov complex. Sample sites: Shubino and Antingan. For Karayanovo samples: see Fig. 2b.

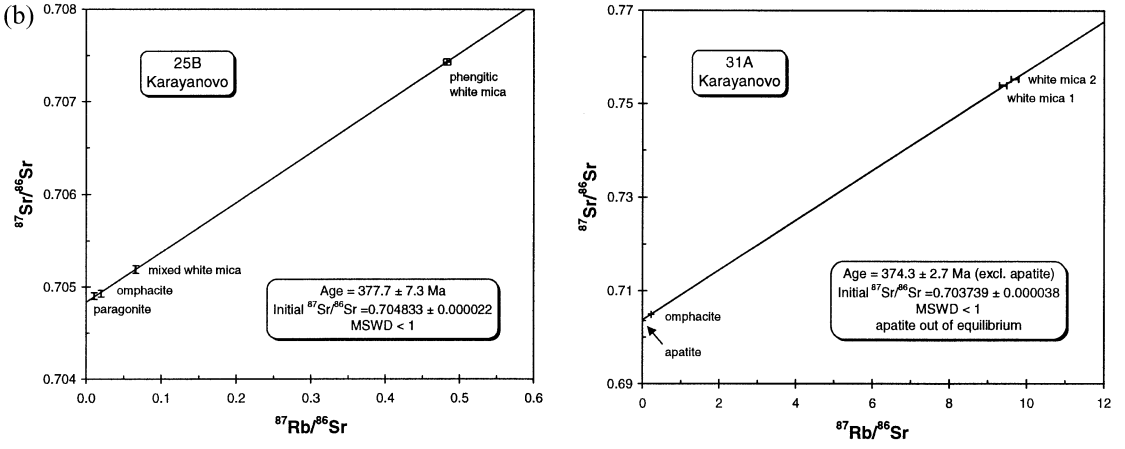

Fig. 2b. Internal mineral isochrons for eclogite-facies rocks, unit #1, Maksyutov complex. Sample site: Karayanovo. For Shubino and Antingan samples: see Fig. 2a.

implies postcrystallization exchange of Sr among mica and the other phases. It has been shown that in rocks with favorable modal composition, mica phases may retain their Rb/Sr characteristics through extreme temperatures, far above the "commonly assumed" closure temperature for mica (Kühn et al., 2000). The dataset of Kühn et al. (2000) furthermore implies that isotope exchange at extreme temperatures may be negligible even for timescales of entire HP metamorphic episodes. In UHP eclogites, zoning of Sr content in epidote acquired during prograde metamorphism is reported, implying that diffusion of Sr in this mineral is slow up to ca. 700°C (Nagasaki and Enami, 1998). For omphacitic pyroxene, a very high blocking temperature for Sr diffusion is expected because of the high ionic bond strengths in its crystal lattice (cf. Dahl, 1997). It can thus be inferred that, at the metamorphic temperatures reached in the Maksyutov complex, these minerals are not open for diffusion and do not act as exchange partners for Sr during regional cooling. In a mafic eclogite matrix, intermineral Sr diffusion is inhibited even at temperatures in excess of 550°C, which is the commonly assumed closure temperature for the Rb/Sr system in white mica (Inger et al., 1996). As a result, the phengite-based Rb/Sr ages can be interpreted as crystallization ages.

Sr isotope exchange after crystallization is also unlikely to have occurred in the quartzitic samples 22E and 23D because

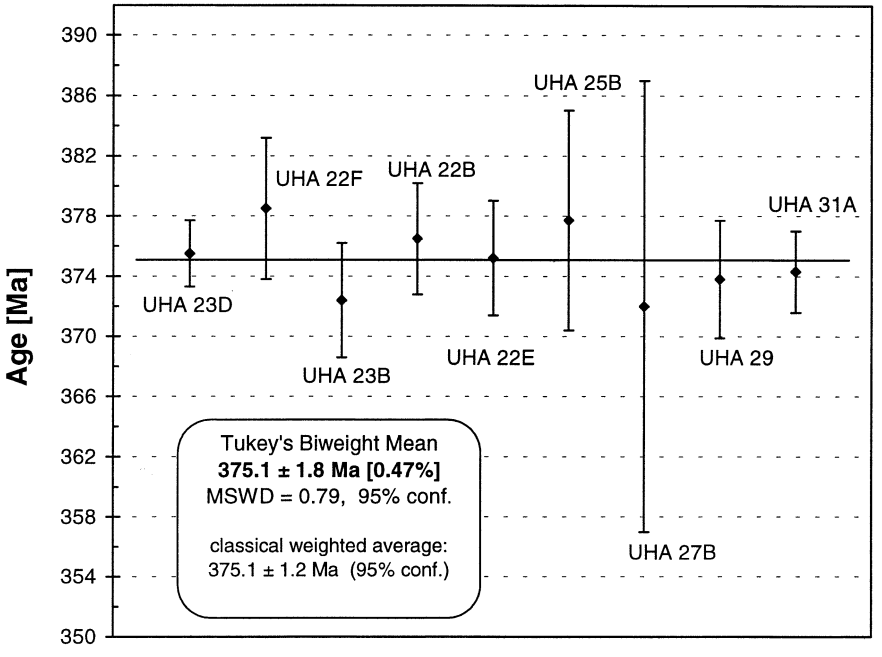

Fig. 3. Summary of age data: Internal mineral isochrons (Rb/Sr) from nine eclogite-facies rocks, unit #1, Maksyutov complex. Calculation of averages with algorithms described in Ludwig (1999). The "Tukey's Biweight Mean" approach assumes dominant normal distribution; assigned errors are ignored. The classical weighted average approach also takes into account individual errors assigned to the age values.

Table 4. Sm/Nd analytical data.

Sample No.	Material	Sm (ppm)	Nd (ppm)	$^{147}Sm/^{144}Nd$	$^{143}Nd/^{144}Nd$	$^{143}Nd/^{144}Nd$ 2σ (%)
23D (Shubino) Apparent age: 416 ± 26 Ma; Nd (i) = 0.51181 ± 0.00004						
OS56	omphacite	1.6508	5.8983	0.1704	0.512272	0.0015
ON4	gamet	4.7874	9.7391	0.2994	0.512623	0.0022
22E (Shubino)						
OS65	epidote	18.3962	56.5756	0.1981	0.512951	0.0024
ON1	gamet	0.1467	0.4421	0.2021	0.512986	0.0023

An uncertainty of ±0.5% has to be assigned to the Sm/Nd ratios. Errors at 2σ level.

of the high quartz content of the rocks (>90% by volume). The other minerals are randomly embedded in the quartz matrix. Due to negligible Rb, Sr abundances, quartz cannot act as a reservoir for isotopic exchange. Instead, quartz has a shielding effect: other minerals had to remain as closed systems for Rb,Sr since the time of crystallization because they were isolated and armored by quartz. Postcrystallization diffusional isotopic exchange between white mica and other phases through the quartz matrix, or by way of the intergranular space, must have been irrelevant because of the diffusion lengths involved, the expected low diffusivities of both elements in the quartz lattice, and the absence of deformation or fluid-triggered retrogression. Therefore, the Rb/Sr age values of eclogitic phases in quartzitic matrix represent crystallization ages.

In the original concept of Dodson (1973), closure temperature is, among other parameters, dependent on effective diffusion lengths. Assuming that grain size is correlated with or equivalent to diffusion lengths, one would expect a positive correlation between mineral grain size and apparent age. In our study, we analyzed different sieve fractions (between 80 and 500 μm, Table 3) of white mica. A significant correlation between grain size and age is not observed. It is concluded that if there was any postcrystallization diffusional readjustment of white mica Rb/Sr-systematics at all, it did not change the original age information significantly.

For sample 23D, a whole rock-omphacite age of 373.7 ± 3.8 Ma can be calculated, in agreement with the ages based on white mica phases. Because omphacitic pyroxene is expected to have a very high blocking temperature for Sr diffusion, this age value is interpreted as dating omphacite crystallization, i.e., the eclogitization reaction in the rock.

The sample pair 22B and 22E represents an eclogite-facies, quartz-rich vein (22E) and the surrounding eclogitic host rock (22B). Mineral isochrons from both lithologies yield identical age values and initial Sr isotopic compositions. This is strong evidence for closed system behavior of the minerals after crystallization. If white mica had been open for diffusional Sr isotopic exchange after crystallization for a prolonged period of time, this exchange process would result in either isotopic disequilibria among phases or an increase of the initial $^{87}Sr/^{86}Sr$ ratio for the rock. The increase would be a function of time and the Rb/Sr ratio in the two whole rocks. In such a case, only in the (unlikely) situation of identical Rb/Sr ratios in both lithologies, would the same initial Sr ratios after final isotopic closure be found. Any difference in Rb/Sr ratios in the whole rocks would result in disequilibrium. Neither mineral nor whole-rock scale disequilibria are observed, indicating closed-system behavior of all phases after crystallization.

Our microprobe analyses show that phengites enclosed in garnets and matrix phengites from the same sample have the same prograde zoning pattern and a similar composition (Table 2, analyses No. 5 to 9). This indicates that all phengite belongs to the primary assemblage formed during the eclogitization reactions. Preservation of prograde zoning rules out postpeak-metamorphic chemical reequilibration. Therefore, Sr-isotopic reequilibration of phengite with its surroundings during cooling and exhumation is highly unlikely. The phengite has preserved its original Rb/Sr system acquired during crystallization.

White mica is highly stable against reopening and recrystallization during retrogression. This is indicated by the results from samples 23B and 27B (Fig. 2) which show that the white micas still record their age of crystallization, whereas the whole rock Rb/Sr systems are disturbed. Because phengite is generally the mineral with the highest Rb/Sr ratio in the rock, any retrograde reopening or recrystallization of phengitic white mica would imply exchange of Sr and thus a less radiogenic signature for the phengite. From altered phengite, anomalously low ages would be expected. The absence of any such rejuvenation demonstrates that, at least in the grain size spectrum selected for this study (>80 μm), all phengites remained inert to posteclogite-facies alteration and their compositions reflect eclogite-facies metamorphism.

Additional evidence for the interpretation of the Rb, Sr isochron data as crystallization ages comes from the observation that in several cases the Mean Square of Weighted Deviates (MSWD) value for the regression calculations is close to 1. The scatter of the data around the regression lines is then explainable by analytical uncertainties alone, indicating absence of additional, “geological” scatter. For single isochrons based on 3 or 4 data points only, the probability of getting an MSWD close to 1 is significant even if some “geological” scatter exists, due to only 1 or 2 degrees of freedom for such regressions. However, the probability of simultaneously obtaining MSWD values close to 1 in multiple isochrons of the same age is negligible. This implies that in our sample set the eclogite-facies phases are in fact in Sr-isotopic equilibrium. Isotopic equilibrium among the minerals of a rock is expected only if either no postcrystallization exchange of Rb, Sr took place or if redistribution of radiogenic Sr was homogeneous or complete. The latter case would imply either the same closure temperature for all minerals of the rock, or temperatures far in excess of the closure temperature of the most Rb, Sr-retentive phase. Both scenarios are implausible, leaving the interpretation as crystallization ages as the only sensible explanation for the good-fit isochrons.

We conclude that the Rb/Sr mineral ages obtained in this study are true crystallization ages.

7.2. Evaluation of the Sm/Nd Data

The apparent age of 416 ± 26 Ma (Sample 23D, Shubino; see Table 4) is in conflict with the well-constrained Rb/Sr crystallization ages. It likely reflects small, but significant Nd-isotopic disequilibria between omphacite and garnet. Such disequilibria are not uncommon in eclogites (Miller and Thöni, 1997) and were also found by Beane and Connelly (2000) in an eclogite sample from the Maksyutov complex. Rare earth elements (REE) may behave as immobile elements during eclogite-facies metamorphism (Arculus et al., 1999), and this may inhibit Nd-isotopic rehomogenization during LT-eclogite-facies metamorphism. Therefore, we interpret the apparent Sm/Nd age as geologically meaningless. However, Nd isotopic disequilibria are not a general feature of the Maksyutov eclogites as indicated by two good-fit (MSWD < 1) Sm/Nd mineral isochrons of Shatsky et al. (1997) (Table 1), the ages of which coincide with our new Rb/Sr ages.

The results of the Sm/Nd analyses allow us to put some constraints on the protoliths of the Maksyutov eclogites: Values for εNd (Chondritic Uniform Reservoir [CHUR]) at the time of metamorphism are +6 for sample 22E and −6 for sample 23D. Shatsky et al. (1997) report values between –1.3 and + 6.3. This variability implies that rocks with fairly different premetamorphic histories (and probably different protolith ages) are present in unit #1 of the Maksyutov complex.

7.3. Fluid–Rock Interaction History

In the Maksyutov complex, free aqueous fluids were present during the eclogitization reactions. This is evident from quartz veining in eclogites (sample pair 22B, 22E) with Sr-isotopic equilibrium between vein and matrix, from abundant garnet veining, the occurrence of atoll-shaped garnets (O'Brien and Carswell, 1997), the complicated epidote growth zoning, and the abundant attainment of textural and Sr-isotopic equilibrium. Furthermore, hydrous phases are ubiquitous in the eclogitic assemblages. Events of fluid activity, caused by influx or internal release, may play an active role in eclogite-facies metamorphism. Fluids trigger and catalyze reactions and growth of eclogite-facies minerals (O'Brien and Carswell, 1997; Austrheim et al., 1997; Scambelluri et al., 1998). This implies that our age data relate to a period of fluid activity under prograde (as inferred from mineral zoning patterns) eclogite-facies conditions. Sr-isotopic equilibria among compositionally zoned minerals indicate that fluid activity was a short-term event. The prograde eclogitization process did not necessarily continue until peak PT conditions. We suggest that the literature data for PT conditions of Maksyutov eclogites in fact reflect the PT conditions of this particular fluid event as the eclogite-facies assemblages were formed at this stage. The absence of retrograde features in large volumes of eclogite testifies that the free fluid was consumed or expelled directly after metamorphism, still under eclogite-facies conditions, leaving a completely dry rock. The local blueschist-to greenschist facies overprint is due to a later episode of fluid influx along fractures and shear zones.

7.4. Cooling and Exhumation Rates

The published rutile U/Pb ages and phengite $^{40}Ar/^{39}Ar$ ages in general overlap with each other, and with the Rb/Sr mineral isochron ages presented here. Beane (1997a) concluded that the overlap of rutile U/Pb ages (interpreted as crystallization ages) and $^{40}Ar/^{39}Ar$ phengite ages (cooling ages) indicates rapid exhumation directly after metamorphism. However, the cooling rates that may be derived by this thermochronology approach are rather uncertain since they are highly dependent on the estimates of closure temperatures. For the K/Ar system in white mica, these estimates range from 350°C to 500°C (Villa, 1998). If the phengite $^{40}Ar/^{39}Ar$ ages are interpreted as close to the metamorphic peak (Matte et al., 1993), no stringent constraints on cooling and exhumation rates at all can be derived from the data discussed here.

However, the Sr-isotopic disequilibria detected in some of our samples require explanation. There is evidence for local retrogression by fluid infiltration and fluid–rock interaction during decompression and cooling, at blueschist- to greenschist facies conditions. The retrogression may occur in one of three contrasted scenarios: (1) largely isochemical retrogression directly after eclogitization, during rapid exhumation; (2) retrogression following eclogitization with a significant delay, with participation of minerals with different Rb/Sr ratios; (3) incomplete retrogression by introduction of fluids, involving metasomatism with respect to Rb and Sr. Scenario 1 would not result in any significant disturbance of the Rb/Sr systematics, whereas scenarios 2 and 3 inevitably lead to Sr-isotopic disequilibria. With the data available, we cannot distinguish between scenarios 2 and 3. Possibly the disequilibria observed in samples 23B, 27B, and 31A have a component of scenario 2. This would suggest that some time (10 to 20 Ma is estimated) elapsed between eclogite-facies metamorphism and the retrogression event at blueschist- to greenschist facies conditions. This estimate is in line with other, more precise constraints on the exhumation history. Investigating exhumation-related mylonites, Hetzel and Romer (2000) concluded that the Maksyutov complex reached midcrustal levels at 360 ± 8 Ma. Age values around 360 Ma were also found by Beane and Connelly (2000) for retrograde shearing. Combining this with our data on the age of eclogitization permits calculation of a "moderate" average exhumation rate of roughly 2 mm/a for the path between 60 and 20 km depth.

7.5. Is There a Stage of Pre-375 Ma Ultra-high-pressure Metamorphism (UHPM)?

Recent papers (Dobretsov et al., 1996; Leech and Ernst, 1998; Leech and Ernst, 2000; Leech and Stockli, 2000) discussed the possibility of an UHPM event in parts of the Maksyutov complex, followed by later HP, eclogite-facies re-equilibration. Ages between pre-400 Ma and 380 Ma were suggested for this UHPM event. The lack of UHP mineral relics was explained by recrystallization on the retrograde path. Several lines of evidence suggest that this hypothesis is not correct.

Prograde fabrics are frequently observed. Epidote, garnet, phengite, omphacite, and amphibole from various samples commonly display prograde growth zoning. These features are

a priori in conflict with models inferring an early distinct UHP stage with later eclogite-facies reequilibration.

Direct evidence for an UHPM event is lacking since no UHP index phases or mineral assemblages were found. Possible findings of coesite and diamond pseudomorphs remain questionable.

Possible prolonged storage at mantle depths, with UHP conditions around 400 Ma and eclogite-facies at 375 Ma, is at variance with the LT signature of metamorphism.

In some of the samples, paragonite occurs as inclusions in garnet and as a matrix phase, associated with phengite showing prograde zoning. Paragonite is a good indicator of maximum pressure as it breaks down via the reaction paragonite = kyanite + jadeite + H_2O. This reaction has been reversed experimentally by Holland (1979), and takes place at 2.5 GPa and 550°C. Since the reaction produces H_2O, kinetic inhibition is unlikely. Furthermore, if the activity of H_2O is <1 in the fluid phase (e.g., if there are ionic solutes, N_2, or CO_2 in the fluid), the breakdown of paragonite will occur at pressures even lower than 2.5 GPa. This indicates that the garnet containing paragonite inclusions grew at pressures below 2.5 GPa, which is the pressure limit for UHP metamorphism as given by the transition quartz-coesite (Bohlen and Boettcher, 1982). The garnet does not record an UHPM event.

Some of the Rb/Sr age data are based on omphacitic pyroxene, a mineral with a presumably high blocking temperature for Sr diffusion. Omphacite is believed to crystallize at some stage of prograde metamorphism; this is *before* (or when) peak-metamorphic conditions are reached. Leech and Ernst (2000) stated, based on textural data, that omphacite, together with garnet, relates to the highest pressure metamorphism. Our omphacite-whole rock Rb/Sr data constrain the age of omphacite crystallization, at a stage of prograde metamorphism, to 374 ± 4 Ma (sample 23D). According to the isotope data, the other eclogite-facies phases are related to this event as well. A pre-375 Ma event is not recorded. Due to the preservation of prograde textural features, a pre-375 Ma UHP equilibration followed by a 375 Ma eclogite-facies reequilibration can be ruled out.

8. CONCLUSIONS

This study demonstrates that internal Rb/Sr mineral isochrons can provide precise age data on crystallization of eclogite-facies assemblages. An unambiguous interpretation of Rb/Sr mineral data requires consideration of several key aspects: All facets of the metamorphic history must be evaluated with respect to their influence on isotope distribution in the rock. In particular, the thermal, the deformational, and the fluid–rock interaction history are important. For determination of crystallization ages by internal Rb/Sr mineral isochrons, favorable settings must be identified in which postcrystallization mobilization of Sr isotopes was possibly inhibited. Such settings are characterized by the absence of late deformation and fluid rock interaction. In rocks with favorable modal composition, e.g., in quartzitic rocks or in mafic eclogites (omphacite, garnet, phengite, ± epidote/zoisite), postcrystallization closed-system behavior of all phases is likely. If, furthermore, indications for diffusional Sr isotope redistribution, such as disequilibria or systematic correlations between grain size and apparent ages are absent, isotope systematics can be interpreted in terms of crystallization ages. Our dataset constrains an age for the eclogitization reactions at 375 ± 2 Ma. This does not define a time-temperature point on the cooling path. We urge caution when using Rb/Sr mineral data for the construction of metamorphic P,T,t paths, to avoid misinterpretation of the results as cooling ages.

Eclogitization was a short-term event, related to fluid activity. This event was part of the prograde metamorphic history, but not necessarily close to the stage of peak-metamorphic PT conditions. The dataset indicates that eclogitization was contemporaneous throughout the entire complex. A pre-375 Ma stage of UHP metamorphism can be ruled out.

Although previous age data for the eclogites cluster around 370 to 380 Ma, in good numerical agreement with the Rb/Sr data, the interpretation and the geological significance of the age data were subject to debate. The Rb/Sr dataset presented here constrains the age of (fluid-mediated) eclogitization to 375 ± 2 Ma. This crystallization age is a clearly defined stage in the metamorphic evolution and therefore represents an anchorpoint for P,T,t-path and geodynamic modeling.

Acknowledgments—This work was funded by a grant of the European Commission (TMR-URO Programme, research network contract No. FMRX-CT96 to 0009 [DG 12-ORGS]). Financial support by the Research Council of Norway (NFR) and by the Nansen Foundation is gratefully acknowledged. We are indebted to V. I. Lennykh and V. Koroteev for excellent expert guidance in the field area. J. G. wishes to acknowledge the support provided by the GeoForschungsZentrum Potsdam for completion of this work. R. Hetzel, R. Romer, K. Gräfe, H. Echtler, and S. Kasemann provided helpful suggestions on an earlier version of the manuscript. Thorough reviews by T. Boundy and an anonymous reviewer are gratefully acknowledged. This is a Europrobe publication.

Associate editor: B. R. Frost

REFERENCES

Amato J. M., Johnson C. M., Baumgartner L. P., and Beard B. L. (1999) Rapid exhumation of the Zermatt-Saas ophiolite deduced from high-precision Sm-Nd and Rb-Sr geochronology. *Earth Planet. Sci. Lett.* **171,** 425–438.

Arculus R. J., Lapierre H., and Jaillard E. (1999) Geochemical window into subduction and accretion processes: Raspas metamorphic complex, Ecuador. *Geology (Boulder)* **27,** 547–550.

Austrheim H., Erambert M., and Engvik A. K. (1997) Processing of crust in the root of the Caledonian continental collision zone: The role of eclogitization. *Tectonophysics* **273,** 129–153.

Beane R. J. (1997a) Ar/Ar evidence for Paleozoic high-pressure metamorphism in the South Urals. In: Geological Society of America, 1997 annual meeting. Abstracts with Programs, *Geological Society of America* **29 (6)**, 399.

Beane R. J. (1997b) Petrologic evolution and geochronologic constraints for high-pressure metamorphism in the Maksyutov complex, south Ural Mountains. Ph.D. dissertation, Stanford Univ., Stanford CA, pp. 1–133.

Beane R. J., and Connelly J. N. (2000) $^{40}Ar/^{39}Ar$, U-Pb, and Sm-Nd constraints on the timing of metamorphic events in the Maksyutov Complex, southern Ural Mountains. *J. Geol. Soc. London* **157,** 811–822.

Beane R. J., Liou J. G., Coleman R. G, and Leech M. L. (1995) Petrology and retrograde P-T path for eclogites of the Maksyutov Complex, southern Ural Mountains, Russia. In: Ultrahigh-pressure metamorphism and tectonics: Proceedings of the first workshop at Stanford University. *The Island Arc* **4 (4),** 254–266.

Berzin R., Oncken O., Knapp J. H., Perez-Estaun A., Hismatulin T., Yunusov N., and Lipilin A. (1996) Orogenic evolution of the Ural Mountains: Results from an integrated seismic experiment. *Science* **274,** 220–221.

Bohlen S. R., and Boettcher A. L. (1982) The quartz<–>coesite transformation: A precise determination and the effects of other components. *J. Geophys. Res.* **B 87,** 7073–7078.

Brown D., Juhlin C., Alvarez-Marron J., Perez-Estaun A., and Oslianski A. (1998) Crustal-scale structure and evolution of an arc-continent collision zone in the southern Urals, Russia. *Tectonics* **17,** 158–171.

Chavagnac V. and Jahn B. M. (1996) Coesite-bearing eclogites from the Bixiling Complex, Dabie Mountains, China: Sm-Nd ages, geochemical characteristics and tectonic implications. *Chem. Geol.* **133,** 29–51.

Chemenda A., Matte P., and Sokolov V. (1997) A model of Palaeozoic obduction and exhumation of high-pressure/low-temperature rocks in the Southern Urals. In *Europrobe's Uralides Project* (eds. A. Perez Estaun, D. Brown, and D. Gee). *Tectonophysics* **276 (1–4)**, 217–227.

Cherniak D. J. (2000). Pb diffusion in rutile. *Contrib. Mineral. Petrol.* **139,** 198–207.

Dahl P. S. (1997) A crystal-chemical basis for Pb retention and fission track annealing systematics in U-bearing minerals, with implications for geochronology. *Earth Planet. Sci. Lett.* **150,** 277–290.

Dobretsov N. L. (1974) Glaucophane Schists and Eclogite-Glaucophane-Schist Complexes in the USSR. *Nauka Press*, Novosibirsk (in Russian).

Dobretsov N. L. and Sobolev N. V. (1984) Glaucophane schists and eclogites in the folded systems of northern Asia. *Ofioliti* **9,** 401–424.

Dobretsov N. L., Shatsky V. S., Coleman R. G., Lennykh V. I., Valizer P. M., Liou J., Zhang R., and Beane R. J. (1996) Tectonic setting and petrology of ultrahigh-pressure metamorphic rocks in the Maksyutov Complex, Ural Mountains, Russia. *Int. Geol. Rev.* **38,** 136–160.

Dodson M. H. (1973) Closure temperature in cooling geochronological and petrological systems. *Contrib. Mineral. Petrol.* **40,** 259–274.

Echtler H. P. (1998) Das südliche Uralgebirge- Tektonik eines intakten paläozoischen Kollisionsorogens. Habilitationsschrift, Universität Potsdam.

Echtler H. P. and Hetzel R. (1997) Main Uralian thrust and main Uralian normal fault: Nonextensional Palaeozoic high-P rock exhumation, oblique collision, and normal faulting in the Southern Urals. *Terra Nova* **9,** 158–162.

Ernst W. G., Liou J. G., and Coleman R. G. (1995) Comparative petrotectonic study of five Eurasian ultrahigh-pressure metamorphic complexes. *Int. Geol. Rev* **37,** 191–211.

Gebauer D. (1990) Isotopic systems: Geochronology of eclogites. In *Eclogite Facies Rocks* (ed. D. A. Carswell), pp. 141–159. Blackie, Glasgow, UK.

Gebauer D., Schertl H. P., Brix M., and Schreyer W. (1997) 35 Ma old ultrahigh-pressure metamorphism and evidence for very rapid exhumation in the Dora Maira Massif, Western Alps. In *High Pressure Metamorphism in Nature and Experiment* (eds. W. Schreyer and B. Stöckhert). *Lithos* **41,** 5–24.

Giletti B. J. (1991) Rb and Sr diffusion in alkali feldspars, with implications for cooling histories of rocks. *Geochim. Cosmochim. Acta* **55,** 1331–1343.

Giletti B. J. and Farver J. R. (1988) Thermal histories of rocks from Rb-Sr mineral data and Sr diffusion kinetics. In: International Congress of Geochemistry and Cosmochemistry (ed. Y. Bottinga). *Chem. Geol.* **70,** 183.

Guidotti C. V., Sassi F. P., Sassi R., and Glencoe J. G. (1994) The effects of ferromagnesian components on the paragonite-muscovite solvus: A semiquantitative analysis based on chemical data for natural paragonite-muscovite pairs. *J. Metamorphic Geol.* **12,** 779–788.

Hamilton W. (1970) The Uralides and the motion of the Russian and Siberian platforms. *Geol. Soc. Amer. Bull.* **81,** 2553–2576.

Hetzel R. (1999) Geology and geodynamic evolution of the high-P/low-T Maksyutov Complex, southern Urals, Russia. *Geol. Rundsch.* **87,** 577–588.

Hetzel R. and Romer R. L. (2000). A moderate exhumation rate for the high-pressure Maksyutov complex, southern Urals, Russia. *Geolog. J.* **35**, 327–344.

Hetzel R., Echtler H. P., Seifert W., Schulte B. A., and Ivanov K. S. (1998) Subduction- and exhumation-related fabrics in the Paleozoic high-pressure-low-temperature Maksyutov Complex, Antingan area, Southern Urals, Russia. *Geol. Soc. Amer. Bull.* **110,** 916–930.

Holland T. J. B. (1979) Experimental determination of the reaction paragonite = jadeite + kyanite + H_2O and internally consistent thermodynamic data for part of the system Na_2O -Al_2O_3 -SiO_2 -H_2O, with applications to eclogites and blueschists. *Contrib. Min. Petrol.* **68,** 293–301.

Inger S., Ramsbotham W., Cliff R. A., and Rex D. C. (1996) Metamorphic evolution of the Sesia-Lanzo zone, western Alps: Time constraints from multi-system geochronology. *Contrib. Min. Petrol.* **126,** 152–168.

Ivanov S. N., Perfilyev A. S., Yefimov A. A., Smirnov G. A., Necheukhin V. M., and Fershtater G. B. (1975) Fundamental features in the structure and evolution of the Urals. *Am. J. Sci.* **275-A,** 107–130.

Jagoutz E. (1995) Isotopic constraints on garnet equilibration. *Terra Abstracts* **7,** 339.

Jenkin G. R. T. (1997) Do cooling paths derived from mica Rb/Sr data reflect true cooling paths? *Geology* **25,** 907–910.

Jenkin G. R. T., Rogers G., Fallick A. E., and Farrow C. M. (1995) Rb-Sr closure temperatures in bi-mineralic rocks: A mode effect and test for different diffusion models. *Chem. Geol.* **122,** 227–240.

Kühn A., Glodny J., Iden K., and Austrheim A. (2000) Retention of Precambrian Rb/Sr phlogopite ages through Caledonian eclogite facies metamorphism, Bergen Arc Complex, W-Norway. *Lithos* **51,** 305–330.

Leech M. L. and Ernst W. G. (1998) Graphite pseudomorphs after diamond? A carbon isotope and spectroscopic study of graphite cuboids from the Maksyutov Complex, south Ural Mountains, Russia. *Geochim. Cosmochim. Acta* **62**, 2143–2154.

Leech M. L. and Ernst W. G. (2000). Petrotectonic evolution of the high-to ultrahigh-pressure Maksyutov Complex, Karayanova area, south Ural Mountains: Structural and oxygen isotope constraints. *Lithos* **52,** 235–252.

Leech M. L. and Stockli D. F. (2000). The late exhumation history of the ultrahigh-pressure Maksyutov complex, south Ural Mountains, from new apatite fission track data. *Tectonics* **19,** 153–167.

Lennykh V. I., Valizer P. M., Beane R., Leech M., and Ernst W. G. (1995) Petrotectonic evolution of the Maksyutov complex, Southern Urals, Russia: Implications for ultrahigh-pressure metamorphism. *Int. Geol. Rev.* **37,** 584–600.

Li S., Wang S., Chen Y., Liu D., Ji Q., Zhou H., and Zhang Z. (1994) Excess argon in phengite from eclogite: Evidence from dating of eclogite minerals by Sm-Nd, Rb-Sr and $^{40}Ar/^{39}Ar$ methods. *Chem. Geol.* **112,** 343–350.

Liou J. G., Wang Q., Zhao M., Zhang R. Y., and Cong B. (1995) Ultrahigh-P metamorphic rocks and their associated lithologies from the Dabie Mountains, central China: A field trip guide to the 3rd international Eclogite field symposium. *Chinese Sci. Bulletin* **40** (Suppl.), 1–71.

Ludwig K. R. (1999) Isoplot/Ex Ver 2.06: A geochronological toolkit for Microsoft Excel. Berkeley Geochronology Center Special Publications, 1a.

Matte P. and Chemenda A. (1996) A mechanism for exhumation of high pressure metamorphic rocks during continental subduction in southern Urals. *Comptes Rendus de l'Academie des Sciences, Serie II. Sciences de la Terre et des Planetes* **323,** 525–530.

Matte P., Maluski H., Caby R., Nicolas A., Kepezhinskas P., and Sobolev S. (1993) Geodynamic model and $^{40}Ar/^{39}Ar$ dating for the generation and emplacement of the high pressure (HP) metamorphic rocks in SW Urals. *Comptes Rendus de l'Academie des Sciences, Serie 2, Mecanique, Physique, Chimie, Sciences de l'Univers, Sciences de la Terre* **317,** 1667–1674.

Mezger K., Hanson G. N., and Bohlen S. R. (1989) High-precision U-Pb ages of metamorphic rutile: Application to the cooling history of high-grade terranes. *Earth Planet. Sci. Lett.* **96,** 106–118.

Miller C. L. and Thöni M. (1997) Eo-Alpine eclogitization of Permian MORB-type gabbros in the Koralpe (Eastern Alps, Austria): New

geochronological, geochemical and petrological data. *Chem. Geol.* **137,** 283–310.
Nagasaki A. and Enami M. (1998) Sr-bearing zoisite and epidote in ultra-high pressure (UHP) metamorphic rocks from the Su-Lu province, eastern China: An important Sr reservoir under UHP conditions. *Am. Mineralogist* **83,** 240–247.
O'Brien P. J. and Carswell D. A. (1997) Phengite growth in an eclogite from the Dabie Mts, China: Early inclusion phase or product of peak P-T fluid influx connected to atoll formation? In: Fifth International Eclogite Conference; Abstracts. *Terra Abstracts* **9** (Suppl. 1), 23.
Reddy S. M., Kelley S. P., and Wheeler J. (1996) A $^{40}Ar/^{39}Ar$ laser probe study of micas from the Sesia Zone, Italian Alps: Implications for metamorphic and deformation histories. *J. Metam. Geol.* **14,** 493–508.
Ruffet G., Feraud G., Balevre M., and Kienast J. R. (1995) Plateau ages and excess argon in phengites: An ^{40}Ar-^{39}Ar laser probe study of Alpine micas (Sesia Zone, Western Alps, northern Italy). *Chem. Geol.* **121,** 327–343.
Ruffet G., Gruau G., Ballevre M., Feraud G., and Philippot P. (1997) Rb-Sr and ^{40}Ar-^{39}Ar laser probe dating of high-pressure phengites from the Sesia Zone (Western Alps): Underscoring of excess argon and new age constraints on the high-pressure metamorphism. *Chem. Geol.* **14,** 1–18.
Scambelluri M., Pennacchioni G., and Philippot P. (1998) Salt-rich aqueous fluids formed during eclogitization of metabasites in the Alpine continental crust (Austroalpine Mt. Emilius unit, Italian Western Alps). *Lithos* **43,** 151–167.
Schulte B. A. and Blümel P. (1999) Prograde metamorphic reactions in the high-pressure metamorphic Maksyutov complex, Urals. *Geol. Rundsch.* **87,** 561–576.
Shatsky V. S., Jagoutz E., and Koz'menko O. A. (1997) Sm-Nd dating of the high-pressure metamorphism of the Maksyutov complex, Southern Urals. *Transactions of the Russian Academy of Sciences/ Earth Science Sections* **353,** 285–288.
Sherlock S., Kelley S., Inger S., Harris N., and Okay A. (1999) ^{40}Ar-^{39}Ar and Rb-Sr geochronology of high-pressure metamorphism and exhumation history of the Tavsanli Zone, NW Turkey. *Contrib. Mineral. Petrol.* **137,** 46–58.
Sobolev N. V., Dobretsov N. L., Bakirov A. B., and Shatsky V. S. (1986) Eclogites from various types of metamorphic complexes in the USSR and the problems of their origin. In *Blueschists and Eclogites* (eds. B. W. Evans and E. H. Brown). Memoir. *Geological Society of America* **164**, 349–363.
Valizer P. M. and Lennykh V. I. (1988) *Amphiboles of blueschists of the Urals*. Nauka Press, Moscow (in Russian)
Villa I. M. (1998) Isotopic closure. *Terra Nova* **10,** 42–47.
Zonenshain L. P., Korinevsky V. G., Kazmin V. G., Pechersky D. M., Khain V. V., and Matveenkov V. V. (1984) Plate tectonic model of the South Urals development. *Tectonophysics* **109,** 95–135.

APPENDIX: SAMPLE PETROGRAPHY

22B. Mafic eclogite, Shubino, 376.5 ± 3.7 Ma

Assemblage: omphacite, phengite, epidote, amphibole, rutile, quartz.

- *Garnet*: rich in inclusions of epidote, blue amphibole, rutile, quartz.
- *Amphibole*: zoning with barroisitic cores to glaucophane rims. Actinolite locally present.
- *Rutile*: without sphene coronas (in contrast to sample 23B).
- *Omphacite*: chemical zoning with increasing Na towards rim.

Sample is crosscut by quartzitic vein (sample 22e).

22E. Quartz vein in eclogite, Shubino, 375.2 ± 3.8 Ma

Assemblage: quartz, phengite, garnet, paragonite, epidote, apatite.

- *Garnet*: displays atoll-shaped habit. Nonsymmetric distribution of MnO in grains near the rim of the vein. Inclusions of epidote and chlorite.
- *Amphibole*: zoning, with barroisitic cores to glaucophane rims.

Quartz vein crosscuts eclogite of sample 22b.

22F. Mafic eclogite, Shubino, 378.5 ± 4.7 Ma

Assemblage: omphacite, epidote, blue amphibole, phengite, quartz, paragonite, rutile.

- *Garnet*: lack the grossularite rich core found in many of the other eclogites. Garnet rim (Alm_{60} $Prp_{22}Grs_{18}Sps_1$), Core ($Alm_{63}Prp_{16}Grs_{20}Sps_{0.8}$). Inclusions of blue amphibole, epidote, quartz, phengite, paragonite.
- *Blue amphibole*: chemical zoning with increasing Fe/Mg ratio and decreasing CaO (1.3 wt.% vs. 0.2 wt.%) towards rim.

Fabric defined by omphacite, epidote, and white mica.

23B. Mafic eclogite, Shubino, 372.4 ± 3.8 Ma

Assemblage: blue amphibole, epidote, omphacite, white mica, garnet, rutile.

- *Garnet*: inclusions of epidote, white mica, rutile. Garnet is fractured. Assemblages in fractures: a) quartz, phengite, epidote, ± glaucophane ± chlorite. b) albite-chlorite.
- *Rutile*: surrounded by sphene when present as matrix phase.
- *Blue amphibole*: primary grains optically zoned, with green, CaO-rich (5 wt.%) cores. Secondary, alteration-related blue amphibole is also present.
- *Phengite*: two generations: primary, and alteration-related. Partly chloritized.
- *Epidote*: zoning, with REE-rich cores; in patches up to 5.5 wt.% SrO. Particularly Sr-rich when enclosed in garnet.

Abundant evidence for alteration under blueschist- to greenschist facies conditions.

23D. Quartzitic eclogite, Shubino, 375.5 + 2.2 Ma

Assemblage: quartz, phengite, garnet, blue amphibole, omphacite.

- *Garnet*: some with atoll shape, no inclusions. In cores: high CaO, low FeO, MgO.
- *Blue amphibole* and *omphacite*: skeletal porphyroblasts without zoning.

25B. Eclogite, rich in quartz and mica, Karayanovo, 377.7 ± 7.3 Ma

Assemblage: quartz, phengite, paragonite, omphacite, garnet, epidote.

- *Epidote*: low in FeO, in contrast to other samples.
- *Omphacite*: with abundant quartz inclusions, locally fringes of actinolite + albite.

27B. Mafic eclogite, Antingan, 372 ± 15 Ma

Assemblage: garnet, rutile, glaucophane, phengite, paragonite.

- *Garnet*: complexly zoned, fractured. Patches with up to 7 wt.% MnO, also patches with Ca-rich garnet ($Alm_{30}Grs_{66}$,Prp_1Sps_3) typically associated with inclusions of paragonite. Abundant inclusions, comprising epidote, actinolite, chlorite, albite, quartz, paragonite, chlorite, sphene, (Ba,Sr)-sulfate, stilpnomelane, omphacite, apatite.
- *Rutile*: surrounded by sphene.

Alteration at blueschist- to greenschist facies conditions. With respect to alteration pattern, the sample in many features resembles sample 23B.

29. Mafic eclogite, Antingan (1 km east of village), 373.8 ± 3.9 Ma

Assemblage: glaucophane, omphacite, quartz, actinolite, phengite, epidote, paragonite.

- *Garnet*: abundant inclusions of paragonite, epidote, chlorite, lawsonite (!), apatite, sphene, omphacite, quartz, stilpnomelane, carbonate. In some grains inclusions are aligned, possibly defining a paleofoliation.

- *Epidote*: locally breakdown to a fine-grained aggregate.

31A. Mafic eclogite, Sakmara river, Karayanovo, 374.3 ± 2.7 Ma
Assemblage: phengite, omphacite, rutile, sphene, garnet.

- *Garnet*: atoll-shaped habit. Profiles from rim toward "lagoon" show an increase in Grs and decrease in Prp, Sps, and Alm. Rim values: $Alm_{70}Sps_{1.6}Grs_{15}Prp_{14}$. Lagoon side: $Alm_{60}Sps_{1.0}Grs_{31}Prp_{7}$.
- *Rutile*: locally surrounded by sphene.